Machine-Learning-Based Health Monitoring & Leakage Management of Water Distribution Systems

Lauren McMillan, Jawad Fayaz, and Liz Varga

Abstract— **Pipe leakage reduction is one of the top priorities of water companies, with many investing in greater sensor coverage to improve the forecasting of flow and detection of leaks. The majority of research on this topic is focused on leakage detection through the analysis of sensor data from district metered areas (DMAs), with the aim of identifying bursts after occurrence. To contribute towards development of 'self-healing' water infrastructural systems, this study applies the concepts of machine-learning and deep-learning to the forecasting of water flow in the DMAs at various temporal scales, aiding in the health monitoring of water distribution systems. The study uses one-year flow dataset of ~2,500 DMAs from Yorkshire. The data contains flow time-series recorded at every 15-minute interval. Firstly, the isolation forest algorithm is used to identify anomalies in the dataset which are verified to correspond to entries in water mains repair log, indicating the occurrence of bursts. Moving beyond leakage detection, this research proposes a hybrid deep-learning-based framework models for flow forecasting at DMA level. A recurrent neural network and Kalman filter provide a mean flow forecast and real-time residual forecast respectively. In addition to providing day-to-day expected flow demands, this framework aims to issue sufficient early warning for any upcoming anomalous flow or possible leakages. For a given forecast period, the framework can be used to compute the probability of flow exceeding a pre-defined threshold, thereby informing decision-making for any necessary interventions. This information can underpin targeted repair strategies to minimise leakage and associated disruption by addressing both detected and predicted burst events.**

Keywords—**Water supply, Leakage, Machine Learning**

I. Introduction

With climate change and rising population levels putting a growing pressure on water supplies, efficient distribution of this increasingly scarce resource is crucial to meeting the needs of consumers within environmental constraints. For 2018-2019, in England and Wales, an average of 3,170 million litres (21% of the water entering the public supply) was lost to daily leakage. This equates to wastage of 53 litres per person per day [1]. A priority for Ofwat, the economic regulator of the water industry in England and Wales, is to reduce leakage across water distribution networks, and recent droughts have driven public interest in how water companies are addressing this crucial issue.

In the UK, it is standard practice for water utility companies to divide their water distribution network into district meter areas (DMAs), with leakage management typically performed at the DMA level [2]. DMAs are groups of up to 2000 households which are isolated section of the water network. Flow is recorded by sensors at the inlet and outlet to each DMA.

Leakage management can be divided into leakage prediction and leakage detection, with the latter being the subject of a significant body of research [3] [4] [5] [6] [7]. Leakage detection models receive data from DMA sensors and try to identify leaks based on changes in the flow profile. The most common methods for identifying leaks utilize the concept of minimum night flows [8]. As night-time water usage is less variable than day-time usage, the average nightly minimum over a specified window can be used as a baseline for comparison with new flow data, and significant variation from this baseline can indicate a leak [9] [10]. However, techniques using minimum night flow have to deal with several uncertainties [8] and rely upon having sufficient knowledge to estimate several parameters including active night users, leakage exponent (which varies with system pressure), and the hour-to-day factor [11]. In reality, while water companies often employ trained operators to try to identify leakage from minimum

Manuscript received 31 August 2022; revised 10 January; accepted 15 January 2023; published 17 July 2023.

This article has been subject to single-blind peer review by a minimum of two reviewers

L. McMillan is with the Infrastructure Systems Institute in the Department of Civil, Environmental, and Geomatic Engineering, University College London (UCL), UK (e-mail: lauren.mcmillan.19@ucl.ac.uk).

J. Fayaz is with the School of Computing, Engineering, and Digital Technologies, Teesside University (TU), UK (e-mail: J.Fayaz@tees.ac.uk). They also hold a position in the Department of Civil, Environmental, and Geomatic Engineering, University College London (UCL), UK.

L. Varga is with the Infrastructure Systems Institute in the Department of Civil, Environmental, and Geomatic Engineering, University College London (UCL), UK (e-mail: l.varga@ucl.ac.uk).

Digital Object Identifier: https://doi.org/10.55066/proc-icec.2022.37

night flow, a significant proportion of leaks are actually reported to water companies by their customers [10].

More recent work conducted in the leakage management and detection domain has explored the potential of using machine learning and deep learning tools. These include artificial neural networks (ANNs) [12] [5] [7], support vector machines [13] [14] [15], Kalman filters (KFs) [16] [17], and wavelet analysis [7]. With sufficient quality and quantity of training data, these methods have demonstrated strong performance in leakage identification [12].

Unlike leakage detection, which is concerned with the identification of leakage events from flow data after they have occurred, the domain of leakage prediction/forecasting aims to anticipate anomalous flow before it occurs, enabling early warning of potential leakage within a given forecasting period. Although leakage detection has observed several dedicated studies, leakage prediction/forecasting has received significantly less attention from the research community due to its complexity. Leakage forecasting at a regional level has been conducted over various time periods ranging from weeks to a year [18], while studies on leakage forecasting at the individual pipe level have analysed pipe properties, such as diameter, age, and material, as well as other factors, including soil type, ground movement, and traffic loading, to assess their impact on leakage likelihood [19] [20] [21]. While not directly applied to leakage, it has been suggested that machine learning techniques, and ANNs in particular, can outperform baseline methods in the forecasting of flow data at the DMA level [22].

Existing work in the area of leakage forecasting is found to be lacking at the DMA level, and the application of sophisticated data-driven machine-learning and deep-learning techniques to this task is scarce, with no instances of advanced time series and sequence modelling. Hence, this study presents a hybrid deep learning framework for leakage forecasting at the DMA level, based on long-short-term memory (LSTM) recurrent neural networks (RNNs) and KF. The framework is trained and tested using an extensive database of one year of 15-minute interval flow data for over 2,500 DMAs. Due to the data-driven nature of the proposed framework, it can be efficiently trained for other DMAs using available flow data and thus can be effectively utilized for proper water resource management.

II. DATASET

This study uses a dataset of over 2,500 DMAs provided by Yorkshire Water, the utility company responsible for water supply and distribution in North Yorkshire, UK. For each DMA, net flow data (in litres/second) is available at 15-minute intervals for a year, from April 2016 to April 2017. Yorkshire Water assigns each flow data to point to a validity code; 'V' for valid, 'I' for invalid, or 'M' for missing, with the vast majority of flow data assigned a 'V'. Fig. 1. shows the flow data for one exemplar DMA. The provided dataset also contains the repair log of the DMAs with their repair dates. Over 5000 repairs are reported in the repair log, covering over 1600 unique DMAs. Repairs are typically prompted either by customer leakage reports or identification of unusual flow data by Yorkshire Water operators, although the repair log does not differentiate between these sources of repair information. While leaks that are customer-reported and visible at surface level are often tackled within a few hours or days, leaks that are not visible may take several weeks to be repaired. The potential for delay between leakage and repair means that a comparison of flow and repair logs alone is insufficient for verifying leakage. Instead, a method is needed for the identification of flow data that likely corresponds to leakage, the timing of which can then be compared to recorded repairs. Repair data, in the absence of widespread metering, is the best alternative for the verification of predicting and identifying leakage events.

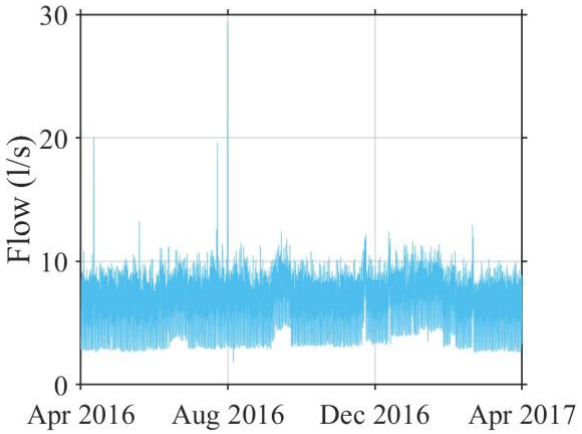

Fig. 1. Flow data for DMA 586

III. METHODOLOGY

The general procedure for training the proposed LSTM-RNN and KF-based framework is illustrated in Fig.2. First, since the sensor data obtained from the DMAs contain missing and invalid flow data points, the flow data is statistically completed using Kalman smoothing. For the completed flow data, the points corresponding to the pipe leakage are identified using the anomaly detection algorithm of isolation forests. As the repair logs do not exactly correspond to the leakage timestamps, it is necessary to use external algorithms to label the most probable leakage points statistically. After the outliers, i.e., the leakage points (denoted as LKG) are identified, for the ~2,500 DMAs, time-series examples of LKG and non-leakage data (represented as NLKG) are appropriately selected. This leads to a total of ~10,000 flow data series for training the proposed framework. As the RNN model requires a consist number of inputs, LKG groups shorter than the maximum are subject to zero-padding. Next, a time-series decomposition is conducted for each of the 10,000 selected flow data series to obtain its trend and seasonal components. These are then used as inputs to train an LSTM-RNN [23], which forecasts the mean flow

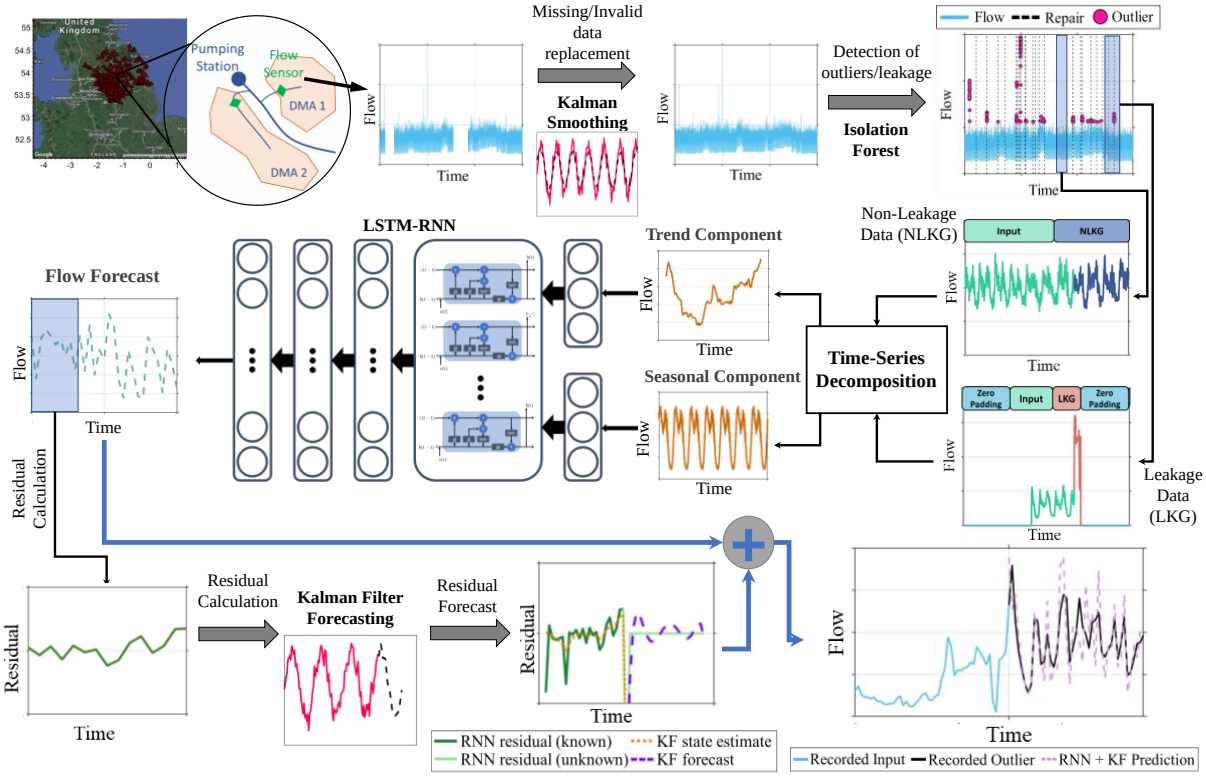

Fig. 2. Procedure for training the proposed LSTM-RNN and KF-based framework

data. The forecasted mean flow data is then used to compute the residuals between the predictions and recorded values of the flow. The residuals are then further used to train a boosting KF that can use residuals in real-time to forecast the future residuals and further improve the predictions. Finally, the forecasted residuals are added to the mean forecast from LSTM-RNN to obtain the final predictions. Hence, the two principal components of the trained framework include 1) LSTM-RNN, which is trained to forecast the expected flow for $t+n$ points using $t-m$ recorded flow, and 2) KF, which provides real-time estimates of residuals and hence shapes the expected predictions of LSTM-RNN closer towards to true flow.

IV. RESULTS

1) *Kalman smoothing for missing/invalid data*

The proposed framework for leakage identification and prediction requires complete flow data. As raw sensor data can be faulty, erroneous sections of flow data are first corrected. Provided the DMA contains sufficient valid data, sections of missing or invalid flow are replaced by the process of Kalman smoothing. This method is found to replace incomplete data with realistic values, with fluctuation from the overall flow curve no more than is seen is the observed adjacent data. Thus, Kalman smoothing allows complete flow data to be provided to the leakage identification model and ensures that the anomaly detection stage of the framework is targeted leakage rather than erroneous data.

2) *Leakage detection and labelling*

Outliers are detected in the completed flow data for all DMAs using the isolation forest algorithm. Fig.3. presents the outliers detected in flow data of an exemplar DMA. The dashed lines in Fig.3. show the dates on which, according to the repair log, the DMA was repaired. The algorithm performs well in identifying both extreme outliers and extended periods of unusual flow rates. The detected outliers, particularly extreme outliers, correlate well with repair dates. Though a small number of repair dates are observed to be away from the outlier data, this can be due to the repairs being conducted for reasons other than pipe leakage, which are not of interest in this study. The algorithm can also flag some other unusual flow data points that do not appear to be leakages. The literature suggests that anomalous flow shorter than a few hours in length is likely not leakage but sensor error, firefighting, or an industrial event [10]. It is therefore important to identify outlier groups such that only extended periods of anomalous flow are flagged as possible leakage, while isolated individual outliers are discarded. For this reason, LKG groupings must be a minimum of 20 outliers in length.

The assumption that outliers in flow data can act as a proxy for real leakage is further validated by comparing the time at which outliers occur and the dates of logged repairs. These times are not expected to directly align, and a degree of fluctuation between the leakage and repair times is expected, as leakage response times can vary depending on factors such as accessibility, size, and visibility. While many operators aim to repair leaks within

a week, this typically refers only to customer-reported leakage. Discussions with industry experts revealed that some leaks can go unrepaired for several weeks, depending on repair priorities.

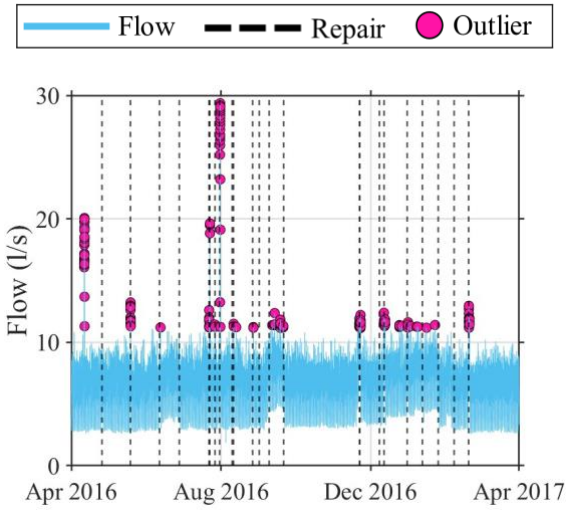

Fig. 3. Outlier identification and repair dates for DMA 586

For DMA 586, which has undergone 22 repairs during the year, it is noted that outliers largely correspond well with recorded repairs, with a significant number of repairs occurring within 24 hours of an outlier. These repairs are likely in response to a customer report of visible leakage. Almost all recorded repairs to DMA 586 took place less than 16 days after a period of outlier flow, with many taking place less than ten days after an outlier. This falls well within the repair timescale that would be expected for less urgent, non-visible leakage or leakage on land requiring permissions for access. These findings confirm that repair data is the best proxy for confirmed leakage events.

Accurate identification of leakage can allow water companies to react effectively to minimize water losses and ensure supply continuation. In this study, the data from identified leakage is also used to train leakage prediction models, which can facilitate the anticipation of leakage and prioritization of preventative maintenance.

3) *Leakage prediction*

A. *Data preparation*

The outlier data provided by the isolation forest algorithm is further processed to ensure it is in a suitable format for training the forecasting framework. Since this study's goal is to forecast both leakage and regular flow data, it is necessary to include both examples leakage groups (denoted as LKG) and non-leakage groups (denoted as NLKG). While the LKG data is obtained via the leakage identification stage of the framework, the NLKG data is randomly sampled from the ~2,300 DMAs in the provided dataset. The size of the LKG and NLKG samples can cause considerable bias in tuning the models, and so after experimentation, a sample size with twice the number of NLKG samples as LKG samples was found to give the best RNN performance.

First, as outlier groupings separated by only a short period of non-outlier flow are likely to represent the same leakage event, outliers within six hours of each other are placed within the same LKG grouping and the interim data points are also labelled as outliers. As literature suggests that short periods of anomalous flow may be due to causes other than leakage [10], the length of each LKG grouping is computed and those with fewer than 20 data points are ignored for this study. The maximum length of LKG data is observed to be 335 points. These LKG groupings will be represented by the outputs of the forecasting stage of the framework. As input to the framework, preceding flow data is required. To have sufficient data for training, this input data needs to be equal to or greater than the LKG data in length. Any LKG groupings where the input data does not meet this requirement are discarded. The maximum length of input data is set to 672 data points, representing a week's flow data, as this is deemed sufficiently long to give a representative sample of flow before an outlier.

Since the RNNs require a set number of input and output data points, all inputs are required to match the maximum length of input, which in this case is 672 data points. For the same reason, all outputs must be 335 in length. For LKG groupings, this consistency is obtained by zero-padding, where zeros are added before the flow data for inputs and after the flow data for outputs (i.e., LKG data). These maximums are also used for the selection of all NLKG data.

Finally, variance checks, using the coefficient of variation (COV), are performed for both LKG and NLKG groupings, to ensure that the selected information is error-free and input data is representative of standard flow. The characteristics of LKG and NLKG groupings are presented in Table I. This dataset is then used to train and test a hybrid forecasting model for leakage prediction.

TABLE I
CHARACTERISTICS OF LKG AND NLKG GROUPINGS

LKG groupings	NLKG groupings
Min 20 datapoints, max 335 datapoints	335 datapoints
Preceding data length >= LKG length, up to a max of 672 datapoints (one week)	Preceding data length = 672 datapoints (one week)
0.1 =< COV =< 10 for input data	0.1 =< COV =< 10 for input data and NLKG data
3,409 groupings	6,818 groupings

B. *Mean flow forecasting*

Additive time series decomposition is used to break down the input data of both LKG and NLKG groupings into a trend, seasonal components, and the remaining noise [24]. The trend component shows the overall pattern of change in flow across a week, while the seasonal

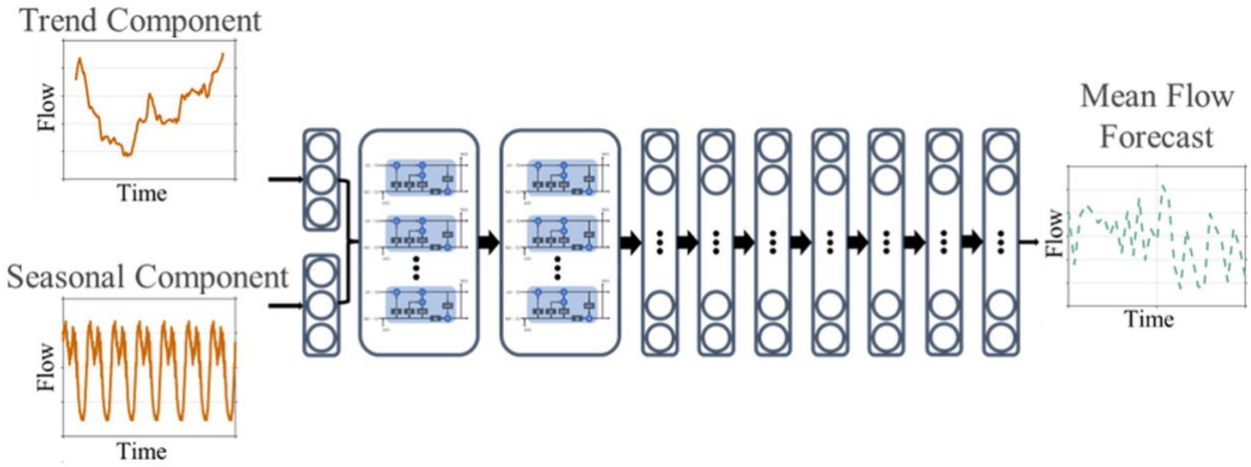

Fig. 4. Architecture of the trained LSTM-RNN

component captures the daily flow pattern. A typical seasonal pattern shows twice-daily peaks and a significant drop overnight, and reflects typical water consumption over 24 hours. Such a pattern is seen in the seasonal component of most input data. The trend component is more variable across LKG/NLKG input groupings, as this is affected by factors such as which (and when) days of the week appear in the data and if and how leakage is reflected in the input data. In order to ensure all relevant patterns are considered, these two components are separately input into the RNN.

The ~10,000 input and LKG/NLKG data groupings are randomly split into train (80%) and test (20%) sets, while making sure train and test sets consists of same ratio of LKG and NLKG data. The train set is used to develop the LSTM-RNN with several configurations and hyperparameters. The training is conducted with 10% cross-validation.

The index of agreement (IA) [25], [26], which has been widely applied to the assessment of model-produced estimates of time-series data [27] [28] [29], is used as the loss function for training and testing the LSTM-RNN, and to compare the accuracy of forecasts before and after the addition of residual forecasting. The calculation of IA is described in Equation 1, where O is the recorded output data and P is the RNN predicted data, and n and i represent the total number of forecasted timesteps and the timestep of interest, respectively.

$$IA = 1 - \frac{\sum_{i=1}^{n}(O_i - P_i)^2}{\sum_{i=1}^{n}(\mid P_i - \bar{O} \mid + \mid O_i - \bar{O} \mid)^2} \quad (1)$$

The best performing final LSTM-RNN architecture in terms of IA is shown in Fig.4. In particular, the LSTM-RNN network is trained using stochastic gradient descent [30] with Adam optimizer [31] and IA [25], [26] as the loss function. Since the values of IA range from 0 to 1, with 1 being the best match and 0 as the worst match, the loss function is used negatively to allow the gradient descent rather than the ascent.

The trained RNN uses flow data's trend and seasonal components as inputs and predicts the flow for future 335-time-steps (i.e., LKG/NLKG data for 335 15-minute intervals). IA values are calculated for each grouping to assess how well these predictions align with the observed LKG/NLKG data. The left part of Fig.5. presents the distribution of IA values for all the groupings. Overall, this IA profile indicates good performance by the RNN, with predicted values and observed flow in good agreement. The vast majority of groupings have an IA value over 0.5, with the first peak between 0.5 and 0.6 and a second, more prominent peak between 0.8 and 0.9. The reason for these peaks may be differences in the 'type' of grouping, so factors that vary between groupings are further investigated. Even at the 25th percentile, the IA value exceeds 0.5, with IA rising to over 0.7 at the 50th percentile. Forecast accuracy, and thus IA values, can be expected to improve with the addition of residual forecasting.

Due to different magnitudes of outliers, LKG groupings vary significantly in length and volatility (i.e., the variance of LKG flow compared to the conflict of preceding input flow). Hence, it is necessary to ensure that the RNN predictions are not biased towards LKG groupings with little volatility compared to the significant volatility groupings. This is done by computing the Z values for the peak flow value in each output grouping (i.e., LKG/NLKG groupings) using Equation 2. In this equation, $peak_{out}$ and $median_{in}$ are the largest value in the LKG/NLKG section of flow and the median value in the input flow, respectively, while σ_{in} is the standard deviation of the input data. The Z value thus compares the size of the output peak to the size and variability of the preceding input data. Computing the Z values and comparing them against corresponding IA values allows the detection of any unintended bias in the model.

$$Z = \frac{\mid (peak_{out} - median_{in}) \mid}{\sigma_{in}^2} \quad (2)$$

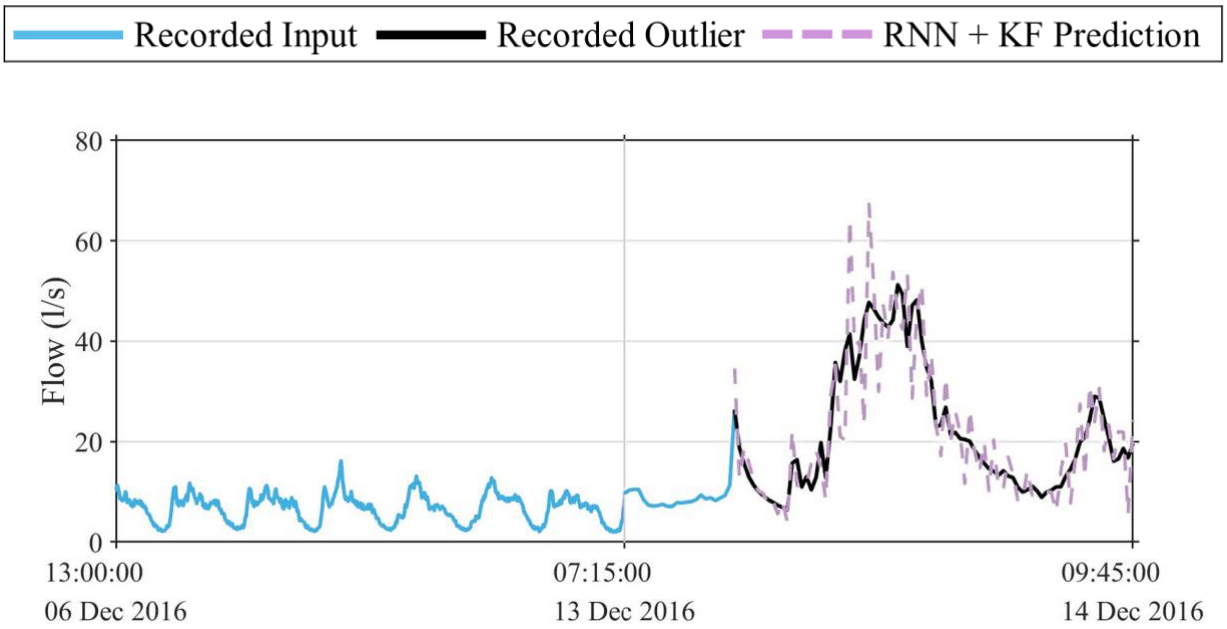

Fig. 6. Forecast for DMA 1316 outlier 1 (IA = 0.9240). Note that the x-axis is split to provide greater detail for the forecasted section of flow In this example, 60 residuals are provided for a forecast window of 24 residuals.

Furthermore, since the LKG/NLKG part of the groupings vary in length and are zero-padded (as described in previous sections), it is essential to check any potential bias in LSTM-RNN predictions concerning the non-zero padded length of the output data. The right side of Fig.5. shows the IA values for all the 10,000 examples compared to the output data's Z values and non-zero padded length. The colour of each dot represents the Z value of each grouping. As the most extended LKG group was 335 data points in length, many groupings possess this length without any zero padding (particularly the NLKG data). While higher values of IA are observed across different LKG group lengths, the concentration of higher Z values in the top left of the plot suggests that the proposed model performs particularly well on leakages with large flow magnitudes and shorter LKG lengths. This may indicate that the preceding flow data for such LKG groups follow a more identifiable pattern captured by the LSTM-RNN. Conversely, the lower IA scores seen in LKG groups with common Z values suggest that the LSTM-RNN struggles to forecast accurately if the peak values are small and the variability in the preceding flow is high.

C. *Residual forecasting*

As the LSTM-RNN model is trained to estimate the mean flow using the known trend and stationary components of the preceding flow, the weights of the LSTM-RNN network are pretrained. They are expected to perform the flow forecasting with known causality. However, to improve the proposed framework's real-time performance, the residuals obtained in the real time are further used to develop state-space model using KF and appropriately forecast the future residuals. Using the pre-trained LSTM-RNN, the flow forecast is obtained from current time t to n time-steps ahead to $t+n$ time, and then as the true values of flow are observed in real-time for time-steps t to $t+k$, where $k<n$, KF is used to model the residuals by finding the difference between the LSTM-RNN forecast and the recorded flow. Due to the recursive nature of KF estimates, this process is expected to provide the framework with real-time deviations of the data and improve the accuracy of the hybrid forecasting system.

As the observed values are considered to be the sum of the underlying state plus noise, KF is performed on known residuals (time-steps $\leq t$) before forecasting so that the prediction can be based on the estimated state rather than the observed values. KF is then used to obtain a forecast for n time-steps ahead. As more data points for the flow are recorded, the residuals are computed, and the updated model is used to forecast the residuals for a future time window. It is observed that forecasting power is improved as more residuals are provided to the model, although this can be verified through checking improvements in IA. The KF demonstrates strong performance in both state estimation of known residual data and forecasting unknown residual data. The state estimation step smooths the observed data, with the estimated states showing less volatility than the observed residual values.

Similarly, while the forecast can predict changes in the overall trend of residual data, many peaks in the observed residual data appear less extreme in the forecasted data. Although huge spikes in residual data may be underestimated in the forecast, the KF effectively captures the overall pattern of residuals. Therefore, adding residual forecasting to mean flow forecasting will allow real-time updates to the forecasting and improve the accuracy of the final combined prediction.

D. *Final flow forecasting*

Finally, the results of mean flow forecasting from the LSTM-RNN and residual forecasting from KF are combined for a final flow forecast. This is presented for an

example case in Fig.6. For the LKG group shown in Fig.6., the LSTM-RNN mean flow forecast has an IA of 0.8466. When combined with the residual forecast, however, the IA for this group rises to 0.9240. This improvement demonstrates the value of this hybrid modelling method. The prediction aligns well with the recorded outlier, anticipating both minor fluctuations and steep changes in flow profile. For example, a drop is seen in both the recorded and predicted lines at the transition to the overnight period. This prediction shows strong agreement with the recorded data throughout the outlier period, not just the overnight section, showing that this method does not require a full day's worth of flow data to identify leakage, unlike many traditional leakage identification methods. Instead, anomalous flow behaviour can be accurately determined and anticipated during daytime hours. This can enable leakage to be flagged more rapidly and thus repairs can be conducted more efficiently.

V. FUTURE WORK

The proposed method could be further optimised by exploring different ratios of LKG and NLKG data. The maximum outlier length could also be cut to see how the model performs with reduced variation in outlier length.

Though currently limited to the DMA level, with additional parameters such as the pipe properties of age, diameter, and material, this work could be extended to address leakage localisation by exploring the prediction of leakage at pipe level. This can then inform targeted repair strategies, as well as contribute to effective preventative maintenance policies. The leakage predicted by either the current method or a pipe level alternative could be linked to a repair prioritisation method. Single-criterion methods may focus on minimising water loss, while other multi-criteria methods may consider other parameters such as water supply to critical infrastructure. By linking the proposed framework with repair scheduling, this work can form part of a 'self-healing' approach to leakage in water distribution systems [32].

VI. CONCLUSION

This study presents a hybrid machine learning-based method for detecting and predicting leakage at the DMA level, which is tested on a database of over 2,500 DMAs managed by Yorkshire Water. For leakage detection, which uses the isolation forest algorithm, results indicate that the outliers identified by the model correlate well with known repairs. This method can flag outliers regardless of the time of day or status of preceding flow data, allowing potential leakage be noticed more rapidly. This may help to raise the proportion of leaks detected first by water companies rather than customers.

For leakage prediction, a LSTM-RNN is combined with KF for flow forecasting. The value of the hybrid approach is validated through the improvements in accuracy provided by the addition of residual forecasting. Leakage prediction is relatively new field of study, and it is hoped that this framework will demonstrate the potential of anticipatory leakage management. Accurate prediction of leakage can allow time-efficient and cost-efficient preventative maintenance, reducing water loss and customer disruption.

REFERENCES

[1] "PR19 final determinations: Securing cost efficiency technical appendix," Ofwat, Dec. 2019. Accessed: Jun. 29, 2021. [Online]. Available: https://www.ofwat.gov.uk/wp-content/uploads/2019/12/PR19-final-determinations-Securing-cost-efficiency-technical-appendix.pdf

[2] J. Morrison, "Managing leakage by District Metered Areas: A practical approach," *Water 21*, pp. 44–46, Feb. 2004.

[3] T. K. Chan, C. S. Chin, and X. Zhong, "Review of Current Technologies and Proposed Intelligent Methodologies for Water Distributed Network Leakage Detection," *IEEE Access*, vol. 6, pp. 78846–78867, 2018, doi: 10.1109/ACCESS.2018.2885444.

[4] R. Puust, Z. Kapelan, D. A. Savic, and T. Koppel, "A review of methods for leakage management in pipe networks," *Urban Water Journal*, vol. 7, no. 1, pp. 25–45, Feb. 2010, doi: 10.1080/15730621003610878.

[5] K. Aksela, M. Aksela, and R. Vahala, "Leakage detection in a real distribution network using a SOM," *Urban Water Journal*, vol. 6, no. 4, pp. 279–289, Oct. 2009, doi: 10.1080/15730620802673079.

[6] Mounce S. R., Boxall J. B., and Machell J., "Development and Verification of an Online Artificial Intelligence System for Detection of Bursts and Other Abnormal Flows," *Journal of Water Resources Planning and Management*, vol. 136, no. 3, Art. no. 3, May 2010, doi: 10.1061/(ASCE)WR.1943-5452.0000030.

[7] M. Romano, Z. Kapelan, and D. A. Savić, "Automated Detection of Pipe Bursts and Other Events in Water Distribution Systems," *Journal of Water Resources Planning and Management*, vol. 140, no. 4, pp. 457–467, Apr. 2014, doi: 10.1061/(ASCE)WR.1943-5452.0000339.

[8] V. J. García, E. Cabrera, and J. Cabrera, "The Minimum Night Flow Method Revisited," pp. 1–18, Apr. 2012, doi: 10.1061/40941(247)35.

[9] P. Malithong, S. Gulphanich, and T. Suesut, "Water loss Control in DMA Monitoring System Used Wireless Technology," 제어로봇시스템학회:학술대회논문집, pp. 773–777, 2005.

[10] S. Mounce, J. Boxall, and J. Machell, "An Artificial Neural Network/Fuzzy Logic system for DMA flow meter data analysis providing burst identification and size estimation," in *Proc. Water Management Challenges in Global Change*, Jan. 2007, p. 320.

[11] P. K. Amoatey, A. A. Obiri-Yeboah, and M. Akosah-Kusi, "Impact of active night population and leakage exponent on leakage estimation in developing countries," *Water Practice and Technology*, vol. 17, no. 1, pp. 14–25, Dec. 2021, doi: 10.2166/wpt.2021.124.

[12] S. R. Mounce and J. Machell, "Burst detection using hydraulic data from water distribution systems with artificial neural networks," *Urban Water Journal*, vol. 3, no. 1, pp. 21–31, Mar. 2006, doi: 10.1080/15730620600578538.

[13] T. Geberemariam, I. Juran, and I. Shahrour, "Virtual DMA Municipal Water Supply Pipeline Leak Detection and Classification Using Advance Pattern Recognizer Multi-Class SVM," *Journal of Pattern Recognition Research*, vol. 9, pp. 25–42, Jan. 2014, doi: 10.13176/11.548.

[14] J. Kang, Y.-J. Park, J. Lee, S.-H. Wang, and D.-S. Eom, "Novel Leakage Detection by Ensemble CNN-SVM and Graph-Based Localization in Water Distribution Systems," *IEEE Transactions on Industrial Electronics*, vol. 65, no. 5, pp. 4279–4289, May 2018, doi: 10.1109/TIE.2017.2764861.

[15] X. Gao, S. Yang, and Y. Hu, "Leakage forecasting for water supply network based on GA-SVM model," in *Proceedings of the 2010 Symposium on Piezoelectricity, Acoustic Waves and Device Applications*, Dec. 2010, pp. 206–209. doi: 10.1109/SPAWDA.2010.5744304.

[16] G. Ye and R. A. Fenner, "Kalman Filtering of Hydraulic Measurements for Burst Detection in Water Distribution Systems," *Journal of Pipeline Systems Engineering and Practice*, vol. 2, no. 1, pp. 14–22, Feb. 2011, doi: 10.1061/(ASCE)PS.1949-1204.0000070.

[17] D. Jung and K. Lansey, "Water Distribution System Burst Detection Using a Nonlinear Kalman Filter," *Journal of Water*

Resources Planning and Management, vol. 141, no. 5, p. 04014070, May 2015, doi: 10.1061/(ASCE)WR.1943-5452.0000464.

[18] L. Birek, D. Petrovic, and J. Boylan, "Water leakage forecasting: the application of a modified fuzzy evolving algorithm," *Applied Soft Computing*, vol. 14, pp. 305–315, Jan. 2014, doi: 10.1016/j.asoc.2013.05.021.

[19] S.-S. Leu and Q.-N. Bui, "Leak Prediction Model for Water Distribution Networks Created Using a Bayesian Network Learning Approach," *Water Resour Manage*, vol. 30, no. 8, pp. 2719–2733, Jun. 2016, doi: 10.1007/s11269-016-1316-8.

[20] K. Jing and Z. Zhi-Hong, "Time Prediction Model for Pipeline Leakage Based on Grey Relational Analysis," *Physics Procedia*, vol. 25, pp. 2019–2024, Jan. 2012, doi: 10.1016/j.phpro.2012.03.344.

[21] N. A. Barton, T. S. Farewell, S. H. Hallett, and T. F. Acland, "Improving pipe failure predictions: Factors affecting pipe failure in drinking water networks," *Water Research*, vol. 164, p. 114926, Nov. 2019, doi: 10.1016/j.watres.2019.114926.

[22] S. R. Mounce, "A comparative study of artificial neural network architectures for time series prediction of water distribution system flow data," in *Machine Learning in Water Systems - AISB Convention 2013*, University of Exeter, UK, 2013, pp. 5–12. Accessed: Jun. 18, 2022. [Online]. Available: https://eprints.whiterose.ac.uk/83574/

[23] J. Fayaz, Y. Xiang, and F. Zareian, "Generalized ground motion prediction model using hybrid recurrent neural network," *Earthquake Engineering & Structural Dynamics*, vol. 50, no. 6, pp. 1539–1561, 2021, doi: 10.1002/eqe.3410.

[24] W. P. Cleveland and G. C. Tiao, "Decomposition of Seasonal Time Series: A Model for the Census X-11 Program," *Journal of the American Statistical Association*, vol. 71, no. 355, pp. 581–587, 1976, doi: 10.2307/2285586.

[25] C. J. Willmott, "On the Validation of Models," *Physical Geography*, vol. 2, no. 2, pp. 184–194, Jul. 1981, doi: 10.1080/02723646.1981.10642213.

[26] C. J. Willmott *et al.*, "Statistics for the evaluation and comparison of models," *Journal of Geophysical Research: Oceans*, vol. 90, no. C5, pp. 8995–9005, 1985, doi: 10.1029/JC090iC05p08995.

[27] G. Duveiller, D. Fasbender, and M. Meroni, "Revisiting the concept of a symmetric index of agreement for continuous datasets," *Sci Rep*, vol. 6, no. 1, Art. no. 1, Jan. 2016, doi: 10.1038/srep19401.

[28] J. Fayaz and C. Galasso, "A generalized ground-motion model for consistent mainshock–aftershock intensity measures using successive recurrent neural networks," *Bull Earthquake Eng*, Jun. 2022, doi: 10.1007/s10518-022-01432-w.

[29] J. Fayaz and F. Zareian, "An efficient algorithm to simulate site-based ground motions that match a target spectrum," *Earthquake Engineering & Structural Dynamics*, vol. 50, no. 13, pp. 3532–3549, 2021, doi: 10.1002/eqe.3521.

[30] J. Kiefer and J. Wolfowitz, "Stochastic Estimation of the Maximum of a Regression Function," *Ann. Math. Statist.*, vol. 23, no. 4, pp. 462–466, 1952.

[31] D. P. Kingma and J. Ba, "Adam: A Method for Stochastic Optimization." arXiv, Jan. 29, 2017. doi: 10.48550/arXiv.1412.6980.

[32] L. McMillan and L. Varga, "Towards self-healing in water infrastructure systems," *Proceedings of the Institution of Civil Engineers - Smart Infrastructure and Construction*, pp. 1–9, Jun. 2022, doi: 10.1680/jsmic.22.00006.